# Spaceborne Radar Interferometry for Landslide Monitoring

L. Cascini & D. Peduto
*University of Salerno, Salerno, Italy*

G. Fornaro, R. Lanari, G. Zeni
*IREA - C.N.R.,Naples, Italy*

F. Guzzetti
*IRPI - C.N.R.,Perugia, Italy*

ABSTRACT: Multipass Differential Interferometry Synthetic Aperture Radar (DInSAR) is gaining an increasing importance for ground deformation monitoring. Compared to classical geodetic techniques such as leveling and GPS it provides advantages in terms of costs, coverage, data accessibility and availability of data archives. As far as landslide phenomena are concerned, the monitoring of surface deformation via the DInSAR technique may provide useful information regarding the spatial and temporal distribution of slow-moving landslides and their kinematics. This work aims to provide an overview of the DInSAR technique to understand the potentialities and the limitations of its applicability to slow-moving landslide monitoring at different scales of analysis. To this end, the results obtained by processing real data of the ERS and Envisat satellites for two case studies are discussed.

## 1 INTRODUCTION

Synthetic Aperture Radar (SAR) is a fine resolution, day-night and all-weather operative remote sensing instrument of key importance in Earth Observation. For more than a decade spaceborne SAR data have been acquired over different tracks, at different times and with varying imaging geometries and stored in space agency archives.

Differential Interferometric Synthetic Aperture Radar (DInSAR) represents a recent advance that makes it possible to widely exploit such data archives. Accordingly, multipass DInSAR is becoming increasingly important as a powerful technique for ground deformation retrieval compared to classical geodetic techniques such as levelling and GPS. It proves superior in terms of costs, coverage, data accessibility and availability of historical archives. So far, applications to monitoring of volcanoes (Massonnet et al. 1995, Borgia et al. 2000), earthquakes (Massonnet et al. 1993, Stramondo et al. 1999), urban areas and infrastructure (Cascini et al. 2006), has been already successfully demonstrated.

Referring to landslide phenomena the application of DInSAR techniques to slope instabilities (Hilley et al. 2004, Colesanti & Wasowski 2006) is a relatively new and still challenging topic. Indeed, efforts are necessary to develop procedures for an enhancement of remote sensing data interpretation based on an in-depth knowledge of the phenomena.

Multipass DInSAR is here revisited to show the potentialities and limitations with respect to the monitoring of landslides at both medium and large scale (according to Fell et al. 2008).

## 2 THE DINSAR TECHNIQUE

The DInSAR technique is based on the concept of interference between SAR images acquired, as much as possible with the same angular view, in repeated passes of the sensor over the same scene. The phase of each SAR images measures, with an accuracy of fractions of the wavelength, the distance of the targets from the sensor.

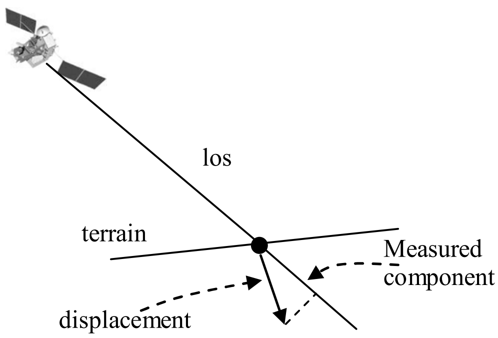


Figure 1: the radar geometry for displacement measurements

Accordingly, the phase of the beating (interference) of the signals acquired in different times provides the measure, again with an accuracy which is a fraction of the wavelength, of the target displacement between the two passes. In particular, referring to Figure 1, the DInSAR technique provides the measure of the component of possible target displacement in the radar line of sight (L.O.S.).

As satellite sensors acquire data over ascending (L.O.S. pointing toward east) and descending (L.O.S. pointing toward west) orbits, two components of the displacement can be measured: the north component is not achievable with the current space-borne technology.

Being rather unlikely to repeat the orbits exactly, interferograms typically contains also the contribution related to the scene topography: the larger the spatial separation (baseline) between the orbits, the higher the contribution of the topography to the interferogram.

Since the first description of the technique (Gabriel et al. 1989) most of the DInSAR applications, which regarded mainly the measurement of displacement associated with earthquakes and volcanoes, were based on the use of a single interferogram (i.e. an image pair) or few interferograms. Products were characterized by: a reduction of the spatial resolution (low resolution interferogram) to improve the phase quality; small baselines to keep low the residual topography contributions.

The advantage of these simple configurations is the flexibility to provide (qualitative) information on deformations, even with a reduced SAR data availability.

Standard two pass DInSAR is limited by the presence of at least two error sources: the APD (Atmospheric Phase Delay) variation and the inaccuracies of the external DEM involved in the cancellation of the topography component from the signal interferences.

The above limitations were overcame for the first time by the Persistent Scatterers (PS) technique (Ferretti et. al 2001) that exploits long acquisition sequences characterized by view and temporal diversity to measure the target displacement and to provide time series of the targets. The PS technique allowed for the first time performing data analysis at full resolution.

At present two classes of techniques are available for multitemporal DInSAR analysis: Persistent Scatterers Interferometry (PSI) and Small BAseline Subset (SBAS) approaches (Berardino et al. 2002).
For the first class, originated by the PS technique, the analysis is carried out at full resolution on stable scatterers in order to separate the atmospheric, topographic and deformation components. Key assumption is the stability of the radar response, which occurs mainly in the presence of dominant point scatterers.

In the case of small baseline techniques, the scattering is supposed to be distributed within the resolution cell and spatial multilooking is implemented to enhance the phase stability. As a consequence of this operation, the spatial resolution is degraded with respect to the PSI approach.

In this sense SBAS approaches are particularly suitable for small scale analysis on wide areas. Nevertheless, a side product of the SBAS small scale analysis is the estimation of the APD component: this feature allows in any case the implementation of a subsequent large scale analysis carried out at full resolution (Lanari et al. 2004, Fornaro et al. 2009a).

As far as the application of multitemporal DInSAR data to landslide studies, the scientific literature (i.e. Colesanti & Wasowski 2006) has widely discussed the current limits:

1) displacement data represent the 1D LOS projection of a deformation that can actually occur in all three dimensions (Rocca 2003, Manzo et al. 2006).

2) The ambiguity of phase measurements implies the impossibility to track correctly and unambiguously a single LOS deformation exceeding $\lambda/4$ (=1.4 cm for ERS) within one revisiting time interval (35 days for ERS), i.e. approximately 14.5 cm/yr, unless a sufficient spatial sampling is provided to spatially integrate the deformation. In practice it is extremely difficult to detect LOS displacement rates exceeding 8–10 cm/yr. This practically limits the use of DInSAR data only to landslides ranging from extremely to very slow phenomena according to the velocity scale of Cruden and Varnes (1996).

3) Limited versatility in terms of (a.) positioning of the measurement points and (b.) revisiting time. Both factors (a.) and (b.) cannot be optimized freely as degrees of freedom while planning an analysis.

4) Finally, it is still difficult to forecast the coherent pixel density in rural areas without carrying out at least several processing steps on a significant number (N15–20) of SAR images.

In this work the limits related to point 2 and point 4 are dealt with, focusing on applications at medium (1:25,000) and large scale (1:10,000).

## 3 MEDIUM SCALE ANALYSIS

The use of low-resolution DInSAR data to study landslide phenomena at medium scale was tested within an area extending for around 489 km$^2$, including eleven municipalities and belonging to the northern portion of the territory of the National Basin Authority of Liri-Garigliano and Volturno rivers (NBA LGV) in Central-Southern Italy (Fig. 2 and Tab.1).

The choice of this area was driven by the availability of both base and thematic maps furnished by the NBA LGV at 1:25,000 scale. These maps were produced in 2001 as results of the activities of the PSAI project (Piano Stralcio per l'Assetto Idrogeologico), carried out by a group of experts and technicians working for NBA LGV in accordance with the Act of Italian Parliament (L. 365/2000), aimed to develop emergency plans at national scale (Cascini 2008).

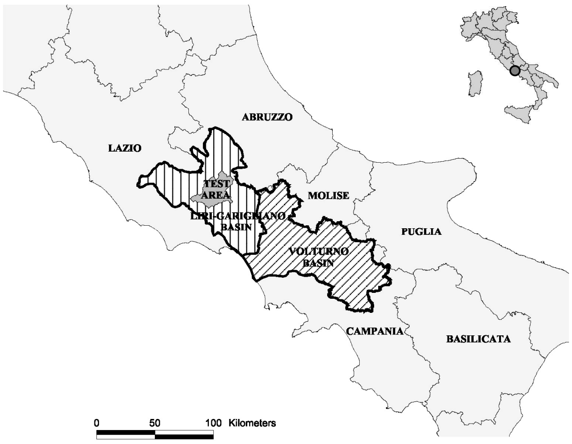


Figure 2. The study area

Table 1. Some data about the study area

| | |
|---|---|
| Total sample area (km$^2$) | 489 |
| Regions | 2 |
| Municipalities | 11 |
| Total Landsliding Area (km$^2$) | 26 |
| Percentage of landsliding area (%) | 5 |

According to the phase ambiguity limitation of DInSAR data processing (point 2 in section 2), the analysis of landslides was focused on the typology of phenomena ranging from *extremely* to *very slow* velocity classes. In the study area a total number of 897 slow-moving landslides are mapped (Peduto 2008, Cascini et al. 2009) and according to Varnes (1978) they are classified as: 204 rotational slides, 238 earth flows, 78 rotational slides-earth flows, 336 creeps, 33 earth flows-creeps, 8 deep-seated gravitational movements.

The DInSAR data analysis was carried out by processing, via the ESD algorithm (Fornaro et al. 2009b), thirty-three images (track 308 - frame 2765) of the European Remote Sensing (ERS-1, ERS2) satellite systems, spanning the time interval from March 1995 until February 2000.

The first step of the analysis dealt with a check of the low-resolution DInSAR data spatial distribution over the whole area (489 km$^2$) at 1:25,000 scale in order to test the limitation reported in point 4 of the previous section.

To this aim, the 17 land-use classes reported in the Map of NBA LGV were homogenized into three main classes exhibiting different scattering properties. Consequently, the classes were ordered, from I to III, according to the expected decreasing likelihood of containing DInSAR coherent pixels. Particularly, Class I (covering 10% of the area) mainly consists of urbanised areas and bare rocks, which are supposed to keep constant their coherence with time. In Class II (covering 43% of the area) cultivated areas and bare soils are included; whereas Class III (covering 47% of the area) groups vegetated areas and inland waters. This last class is expected to be the worst in terms of DInSAR pixel coherence keeping.

Subsequently, the number of low-resolution DInSAR ESD coherent pixels as well as their density (the number of coherent pixels per square kilometre) were computed for each Class. The obtained results (Fig.3) show that the majority of coherent pixels concentrates on Class II and Class I areas (i.e. cultivated and urbanised, respectively), but the highest density is attained in Class I areas (more than 63 coherent pixels per km2); far lower density values are attained in Class III areas (6.16 pixels per km$^2$).

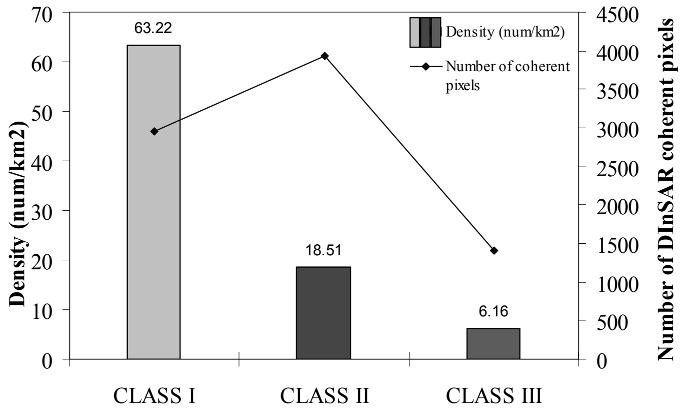


Figure 3. Density and number of DInSAR coherent pixels for the three different classes (Peduto, 2008).

On the whole, it is confirmed that an adequate DInSAR coherent pixel distribution is difficult to be achieved over densely vegetated area; conversely, the remote sensing information concentrate on built-up areas and bare rocks.

This constraint affects the number of landslides covered by DInSAR data. In order to investigate this aspect, the low-resolution ESD DInSAR coherent pixel (with areas of around 80 x 80 m) map was overlaid on the Landslide Inventory Map and one single mapped phenomenon was assumed to be "covered" if at least one low-resolution coherent pixel was found on it. Accordingly, the low-resolution DInSAR data coverage for each mapped landslide typology was derived (Fig.4).

Considering that DInSAR data were processed only on descending orbit, it can be noticed that 301 slow-moving landslide phenomena resulted covered by low-resolution DInSAR data. This corresponds to an average percentage of around 34% out of the total of 897 landslides and creeping phenomena mapped within the territory of the 11 investigated municipalities.

DInSAR mean velocity values, derived from displacement time series computed along the LOS direction, were then used as ground surface movement indicators for the observation period at hand. Particularly, it was assumed a displacement rate threshold of 1.5 mm/year for conditions of movement (values higher than 1.5 mm/year) or no-movement (values lower than 1.5 mm/year). This threshold, based on experimental evidences, was selected as a conservative rate of the average displacement (Colesanti et al. 2003).

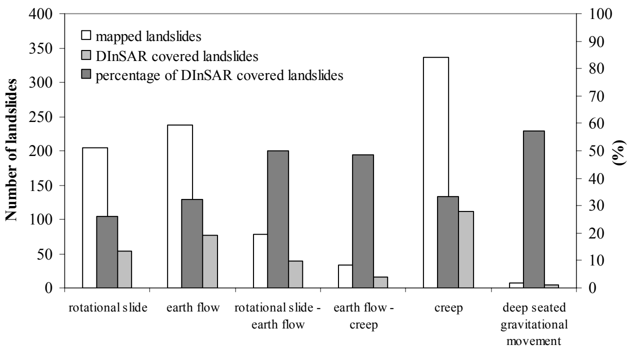


Figure 4. Low-resolution DInSAR data coverage on Landslide Inventory Map (Peduto, 2008).

The setting of the above mentioned threshold allowed the detection of displacements within each SAR covered landslide whose activity state is defined in the Landslide Inventory Map on the basis of geomorphological criteria.

This analysis was carried out with reference to rotational slides, earth flows and rotational slides-earth flows whose total amount in the study area is 520; 169 (around 32%) of those resulted covered by DInSAR data.

Accordingly, Figure 5 shows that almost 84% of the SAR covered dormant landslides (144) exhibited evidence of no-movement. On the other hand, the percentage of active landslides (25) with moving coherent DInSAR pixels is about 24%, on the average.

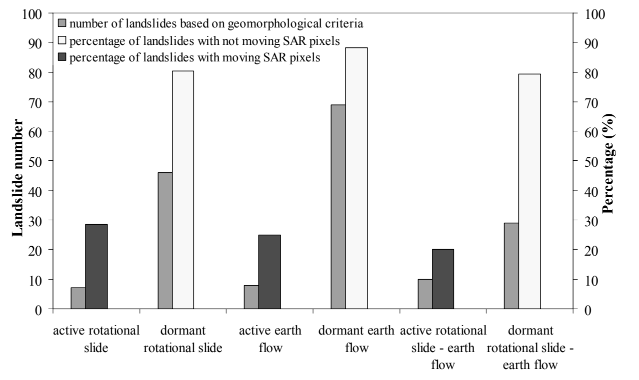


Figure 5. Evidence of movements within inventoried phenomena (Peduto, 2008).

These data outline the possibility of using the DInSAR techniques for checking/updating the Landslide Inventory Map.

Another possibility arises analysing those portions of the territory mapped as hollows on the Geomorphological Map (1:25,000 scale) of the NBA LGV. Actually, these zones are not classified as landslides but they are characterized by geomorphological settings quite similar to landslide affected areas, also exhibiting the same landslide predisposing factors.

Accordingly, the low-resolution DInSAR moving/not moving coherent pixel map overlaid on the Geomorphological Map allowed the detection of 63 (out of 1261) hollows where evidences of movement were recorded.

In Figure 6 an example of mapped landslide phenomena, DInSAR coherent pixels and hollows is reported, distinguishing with horizontal hatch the hollows where movements were detected by DInSAR data analysis.

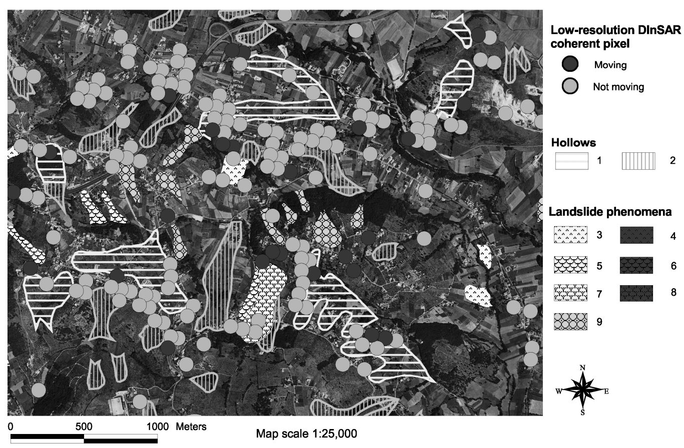


Figure 6. An example of detection of low-resolution moving DInSAR coherent pixels within portions of the territory mapped as hollows. 1) Hollow with moving DInSAR coherent pixel; 2) Hollow not covered or with not moving DInSAR coherent pixel; 3) dormant rotational slide; 4) active rotational slide; 5) dormant earth flow; 6) active earth flow; 7) dormant rotational slide – earth flow; 8) active rotational slide – earth flow; 9) creep phenomenon (Peduto, 2008).

## 4 LARGE SCALE ANALYSIS

The analysis at large scale was developed via the full-resolution SBAS technique (Lanari et al., 2004) in order to retrieve mean deformation velocity maps and associated times series for selected areas within the territory of Umbria Region, Central Italy (Fig. 7). For this area, a detailed landslide inventory map is available in digital format. The inventory was prepared at 1:10,000 scale through the interpretation of stereoscopic, vertical aerial photographs taken at scales ranging from 1:13,000 to 1:33,000 in the period from 1954 to 1977, aided by limited field checks (Guzzetti et al. 2003). Landslides revealed in the inventory map are mostly of the slide, earthflow, complex, and compound types (Cruden & Varnes 1996), and cover about 10% of the hills and the mountains of the study area. Historical information (Guzzetti et al. 2003, Salvati et al. 2006) and field evidence (Felicioni et al., 1994) suggest that most of the mapped landslides are dormant, and that the active ones move slowly to very slowly. Several landslides affect urban areas and roads (Felicioni et al. 1994). Among these, the Ivancich area in the Assisi Municipality, affected by a slow moving, deep-seated landslide of the slide type - extending for about $3\times10^5$ m$^2$ (Canuti et al. 1986) - was analysed. This phenomenon repeatedly caused damage to roads, buildings, and retaining structures (Felicioni et al. 1994).

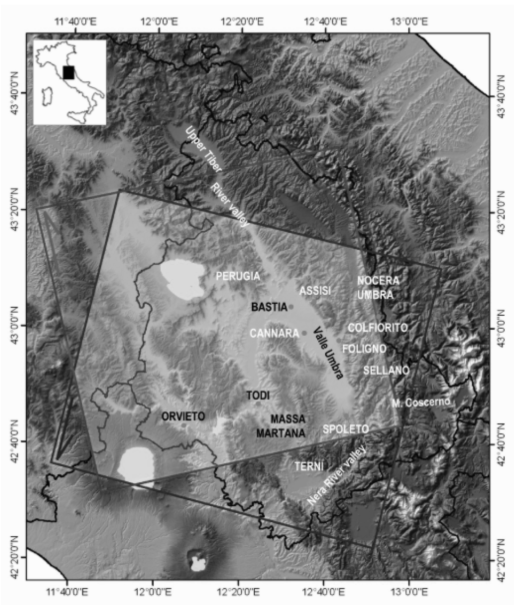


Figure 7. Map showing terrain morphology in Umbria, central Italy. Inset shows approximate location of the study area. Two boxes show extent of ERS-1/2 footprint for track 172, frame 855 (ascending orbit) and footprint for track 351, frame 2745 (descending orbit).

The processed SAR dataset consisted of 24 images of ERS-1 and 2 satellites, acquired along ascending orbit (track 172, frame 855) in the period between June 1995 and November 2000 and 49 SAR acquisitions along descending orbits (track 351, frame 2745) in the period from April 1992 to December 2000 (Fig. 7).

The full-resolution DInSAR data (Fig. 8) reveals a good agreement between the location of the landslide and the position of SAR pixels, thus confirming the spatial pattern of ground deformations.

Moreover, this map allow the identification of a specific sector of the landslide in which the highest displacement rates were recorded during the investigated period, and the precise location of the boundaries of the active landslide area.

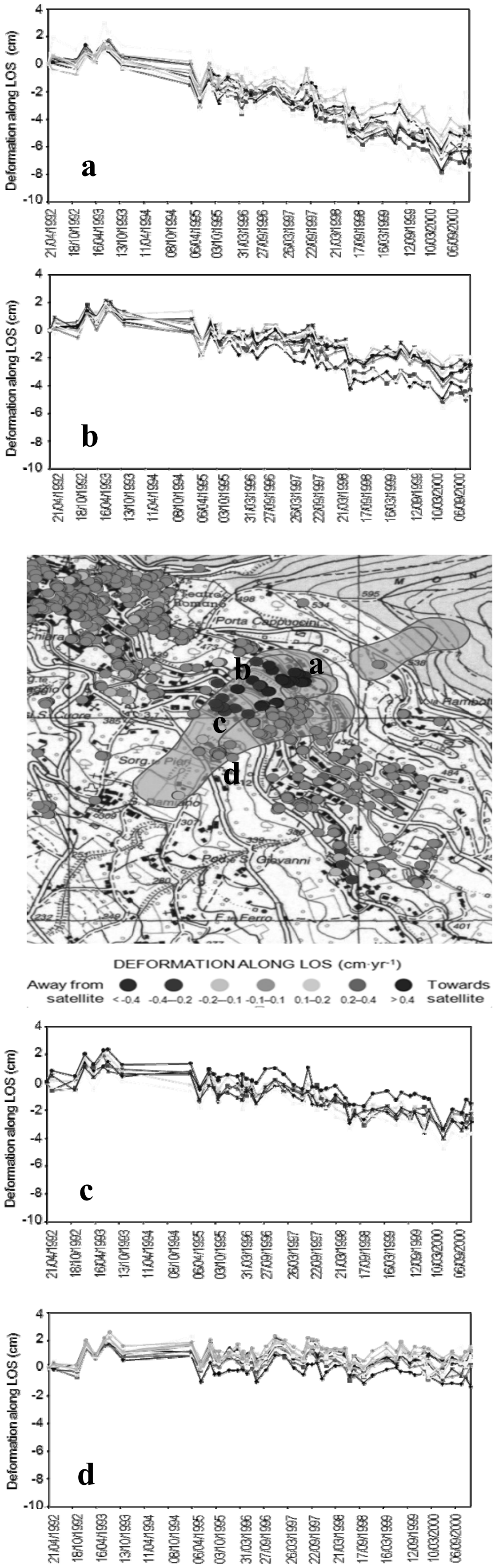


Figure 8. Temporal pattern of the topographic deformation measured through the SBAS-DInSAR technique in the Ivancich area, Assisi Municipality. Deformation along LOS shown in cm for four areas in the landslide deposit.

Particularly, the interpretation of the deformation plots suggests the following considerations: (a) displacements were higher in the upper part of the failed slope, near the landslide crown area, (b) the deformation was less intense in the central part of the active landslide area, and reduced further down slope.

Moreover, the pattern of deformation is in agreement with the location of buildings, roads, and retaining walls that suffered damage in the Ivancich zone (Felicioni et al., 1994) (Fig. 9). Particularly, most of the damaged structures are located in areas where displacements detected by DInSAR technology were higher than 4 cm along the L.O.S. direction during the observation period (1992 – 2000).

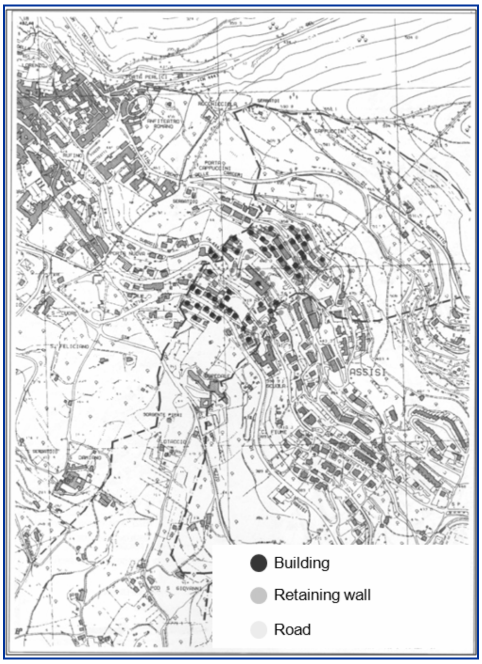


Figure 9. Map showing damage to buildings, roads, and retaining structures (modified after Felicioni et al. (1994)

## 5 CONCLUSION

Landslide monitoring via conventional techniques can turn out to be extremely expensive and time consuming especially over large areas. In this regard, the use of remote sensing data, such as those derived by DInSAR techniques, can provide researchers with a huge amount of data whose reliability is increasingly growing in the last years. In this work the potentialities and the limitations associated with use of DInSAR in landslide monitoring are discussed.

The first analyzed test case shows that the percentage of landslides covered by radar measures is around 30% of the total number of slow-moving landslides. This is a direct consequence of the vegetation that introduces random variation of the scene radar response and of the sensor acquisition geometry, which limits the visibility to portions of slopes. Despite this coverage limitation, DInSAR measurements are valuable over large areas, mostly when ground truths are lacking.

Particularly, low-resolution DInSAR data can be used for landslide analyses at medium scale (i.e.1:25,000 scale) to derive elements to check/update Landslide Inventory Maps within the visible areas; whereas full-resolution DInSAR data allow studies at more detailed scale (i.e. 1:10,000 and higher) furnishing an insight into the main features and kinematics of a single phenomenon and into the behaviour of the buildings \ infrastructures involved by landsliding.

Accordingly, current advances in research are necessary in order to develop standardized procedures for a confident use of DInSAR data in landslide monitoring. These advances could be facilitated by many sensors operating at different frequencies already orbiting around the Earth and characterized by very high spatial resolution features (e.g. Italian Cosmo Skymed constellation) and reduced revisiting time.

## ACKNOWLEDGEMENTS

The Authors are grateful to National Basin Authority of Liri–Garigliano and Volturno rivers for furnishing base and thematic maps as well as SAR images and damage database related to the study area.

## REFERENCES

Berardino P., Fornaro G., Lanari R. and Sansosti E. 2002. A New Algorithm for Surface Deformation Monitoring based on Small Baseline Differential SAR Interferograms. *IEEE Trans. Geosci. and Remote Sens.* 40 (11): 2375-2383.

Borgia, A., Lanari, R., Sansosti, E., Tesauro, M., Berardino, P., Fornaro, G., Neri, M., Murray, J. 2000. Actively growing anticlines beneath Catania from the distal motion of Mount Etna's decollement measured by SAR interferometry and GPS. *Geophysical Research Letters* 27(20): 3409-3412.

Canuti, P., Marcucci, E., Trastulli, S., Ventura, P., and Vincenti, G. 1986. Studi per la stabilizzazione della frana di Assisi. *National Geotechnical Congress, Bologna, 14-16 May 1986,* Vol. 1, 165-174.

Cascini L. 2008. Applicability of landslide susceptibility and hazard zoning at different scales. *Engineering Geology* 102 (3-4): 164-177.

Cascini L., Ferlisi S., Fornaro G., Lanari R., Peduto D., Zeni G. 2006. Subsidence monitoring in Sarno urban area via multitemporal DInSAR technique. *International Journal of Remote Sensing* 27(8): 1709-1716.

Cascini L., Fornaro G., Peduto D. 2009. Analysis at medium scale of low-resolution DInSAR data in slow-moving landslide affected areas. Submitted to *ISPRS Journal of Photogrammetry and Remote Sensing*.

Colesanti C., Wasowski J. 2006. Investigating landslides with space-borne Synthetic Aperture Radar (SAR) interferometry. *Engineering Geology* 88: 173–199.

Cruden D.M., Varnes D.J. 1996. Landslide types and processes. In: Turner, A.K. and Schuster, R.L. (eds.) *Land-*

*slides, Investigation and Mitigation, Transportation Research Board Special Report 247,* Washington D.C., 36-75.
Felicioni, G., Martini, E. and Ribaldi, C. 1994. *Studio dei Centri Abitati Instabili in Umbria*. Rubettino Publisher, 418 p. (in Italian).
Fell R., Corominas J., Bonnard C., Cascini L., Leroi E., Savage W.Z. 2008. Guidelines for landslide susceptibility, hazard and risk zoning for land-use planning. *Engineering Geology* 102 (3-4): 99-111.
Ferretti A., Prati C., and Rocca F. 2001. Permanent scatterers in SAR interferometry, *IEEE Trans. Geosci. and Remote Sens.* 39 (1): 8–20.
Fornaro G., Pauciullo A., Serafino F. 2009b. Deformation monitoring over large areas with multipass differential SAR interferometry: A new approach based on the use of spatial differences, *International Journal of Remote Sensing*, April, 000.
Fornaro G., Reale D., Serafino F. 2009a. 4D SAR Imaging for Height Estimation and Monitoring of Single and Double Scatterers", *IEEE Transactions on Geoscience and Remote Sensing* 47 (1): pp. 214-223.
Gabriel K., Goldstein R. M., Zebker H. A. 1989. Mapping small elevation changes over large areas: Differential interferometry, *J. Geophys. Res.* 94.
Guzzetti, F., Reichenbach, P., Cardinali, M., Ardizzone, F., and Galli, M. 2003. The impact of landslides in the Umbria Region, Central Italy. *Natural Hazards and Earth System Sciences 3:5*, 469-486.
Guzzetti, F., Ardizzone, F., Cardinali, M., Galli, M., and Reichenbach, P. 2008. Distribution of landslides in the upper Tiber River basin, central Italy. *Geomorphology* 46(1-2): 105-122.
Hilley G.E., Burgbman R., Ferretti A., Novali F., Rocca F. 2004. Dynamics of slow-moving landslides from Permanent Scatterer Analysis. *Science* 304: 1952-1955.
Lanari, R., Mora, O., Manunta, M., Mallorquì, J.J., Berardino, P., and Sansosti, E. 2004. A Small Baseline Approach for Investigating Deformations on Full resolution Differential SAR Interferograms. *IEEE Transactions on Geoscience and Remote Sensing 42*, 1377-1386.
Manzo M., Ricciardi G.P., Casu F., Ventura G., Zeni G., Borgstrom S.,Berardino P. , Del Gaudio C., Lanari R. 2006. Surface deformation analysis in the Ischia Island (Italy) based on spaceborne radar interferometry. *Journal of Volcanology and Geothermal Research* 151: 399–416.
Massonnet, D., Briole, P., Arnaud, A., 1995. Deflation of Mount Etna monitored by Spaceborne Radar Interferometry, *Nature* 375: 567-570.
Massonnet, D., Rossi, M., Carmona, C., Adragna, F., Peltzer, G., Feigl, K., Rabaute, T. 1993. The displacement field of the Landers earthquake mapped by radar interferometry. *Nature* 364: 138-142.
Peduto D. 2008. *Analysis of ground deformations related to subsidence and landslide phenomena via DInSAR techniques.* Ph.D.Thesis University of Salerno, Italy, May 2008. Tutor: Prof. Cascini L.; co-tutor: Dr.G.Fornaro.
Rocca, F. 2003. 3D Motion recovery with multi-angle and/or left right Interferometry. Proceedings of the *Third InternationalWorkshop on ERS SAR Interferometry (FRINGE 2003)*, Frascati (Italy), 2–5 December 2003. ESA SP-550, available also online: http: //earth.esa.int /fringe03/ proceedings/ (accessed 23 April 2009).
Salvati, P., Bianchi, C., and Guzzetti, F. 2006. *Catalogo delle Frane e delle Inondazioni Storiche in Umbria*. CNR IRPI e Fondazione Cassa di Risparmio di Perugia, ISBN-10 88-95172-00-0, ISBN-13 978-88-95172-00-2, 278 p. (in Italian).
Stramondo, S. , M. Tesauro, P. Briole, E. Sansosti, S. Salvi, R. Lanari, M. AnzideiI, P. Baldi, G. Fornaro, A. Avallone, M. F. Buongiorno, G. Franceschetti, E. Boschi, 1999. The September 26, 1997 Colfiorito, Italy, Earthquakes: Modeled Coseismic Surface Displacement from SAR Interferometry and GPS. *Geophysical Research Letters* 26(7): 883-886.


# RAINFALL-INDUCED LANDSLIDES

## mechanisms, monitoring techniques and nowcasting models for early warning systems

Volume 1

E. Alonso, N. Pinyol
H. Rahardjo, R.B. Rezaur, E.C. Leong
L. Cascini, S. Cuomo, S. Ferlisi, G. Sorbino
M. Castelli, S. Duca, G. Pisani, C. Scavia
A. Graziani, T. Rotonda, P. Tommasi
O. Hungr
S. Leroueil, J. Chu, D. Wanatowski
C.W.W. Ng
A. Spickermann, J.P. Malet, Th.W.J. van Asch
L. Zeni
G. Alberti, L. Ciofaniello, G. Galiero, G. Palmese
L. Boccia, G. Amendola, G. Di Massa
L. Cascini, D. Peduto, G. Fornaro, R. Lanari, G. Zeni, F. Guzzetti
S. Costanzo, G. Di Massa, F. Venneri
Th.W.J. van Asch, L.P.H. Van Beek, T.A. Bogaard
M.T. Brunetti, S. Peruccacci, M. Rossi, F. Guzzetti, P. Reichenbach, F. Ardizzone, M. Cardinali, A. Mondini, P. Salvati, G. Tonelli, D. Valigi, S. Luciani
G. Capparelli, D. Biondi, D.L. De Luca, P. Versace
J.L. Durville, J. Kasperski, J.P. Duranthon
M. Giorgio, R. Greco, G. Capparelli, P. Versace
L. Laloui, A. Ferrari, Ch. Bonnard
A. Ledesma, J. Corominas, D.A. González, A. Ferrari
F. Nadim, J. Cepeda, F. Sandersen, C. Jaedicke, H. Heyerdahl
L. Pagano
M. Pastor, D. Manzanal, T. Blanc, M. Sánchez, J.A. Fernández Merodo, P. Mira, V. Drempetic
P. Schiano, P. Mercogliano, L. Comegna
D. Znidarcic, J. Lee

Editors: Luciano PICARELLI Paolo TOMMASI Gianfranco URCIUOLI Pasquale VERSACE

UNICAL
CAMI Lab. di Cartografia Ambientale e Modellistica Idrogeologica
CIRIAM Centro Interdipartimentale di Ricerca in Ingegneria Ambientale
Seconda Università degli Studi di Napoli
DIGA Dipartimento di Ingegneria Idraulica Geotecnica ed Ambientale
Dipartimento di Ingegneria Strutturale e Geotecnica
SAPIENZA Università di Roma